Soft Periodic Microstructures Containing Liquid Crystals

ARTICLE *in* THE JOURNAL OF PHYSICAL CHEMISTRY B · JANUARY 2013

Impact Factor: 3.3 · DOI: 10.1021/jp311027p · Source: PubMed

THE JOURNAL OF PHYSICAL CHEMISTRY B

Article

pubs.acs.org/JPCB

Soft Periodic Microstructures Containing Liquid Crystals

Luciano De Sio,*[,†] Sameh Ferjani,[‡] Giuseppe Strangi,[†,§] Cesare Umeton,[†] and Roberto Bartolino[†]

[†]Department of Physics and Centre of Excellence for the Study of Innovative Functional Materials, University of Calabria, CNR-IPCF UOS Cosenza, 87036 Arcavacata di Rende (CS), Italy

[‡]Radiation Oncology, Cleveland Clinic, 9500 Euclid Avenue, Cleveland, Ohio, 44195, United States

[§]Department of Physics, Case Western Reserve University, Cleveland, Ohio 44106, United States

Supporting Information

ABSTRACT: An empty polymeric structure has been realized by combining a high precision level optical holographic setup and a selective microfluidic etching process. The distinctive features of the realized periodic microstructure enabled aligning several kinds of liquid crystal (LC) compounds, without the need of any kind of surface chemistry or functionalization. In particular, it has been possible to exploit light sensitive LCs for the fabrication of all-optical devices, cholesteric and ferroelectric LCs for ultrafast electro-optical switches, and a common LC for a two-dimensional periodic structure with high anisotropy. All-optical and electro-optical experiments, performed for investigating the samples in terms of switching voltages and response times, confirm good performances of the realized devices.

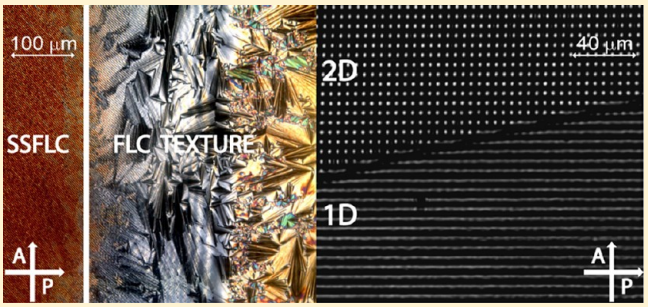

INTRODUCTION

Liquid crystals (LCs) are self-organizing dielectric soft materials that possess both order and mobility at molecular, supramolecular, and macroscopic levels. They are very attractive, due to a wide range of applications, spanning from optics to telecom. LCs exhibit an extreme sensitivity to small external perturbations such as electric, optical, magnetic fields, and surface effects, which is the basis for their information and display application. They currently play a significant role in nanoscience and nanotechnology too; in particular, LCs can be utilized in nanoscience, thus realizing a bridge between "hard matter" and "soft matter", because nanostructurated materials do not induce significant distortions of LC phases. In fact, various nanomaterials have been dispersed and studied in LCs to enhance their physical properties; in addition, alignment and self-assembly of nanomaterials themselves can be achieved in LC phases. Indeed, LCs act as tunable solvents for the dispersion of nanomaterials and, being anisotropic media, they provide a good support for the self-assembly of those materials into large organized structures, even in multiple dimensions. Alignment of the LC molecular director represents, therefore, a key issue in the framework of LC-based photonic devices and, in order to realize this goal, in the past decades a variety of aligning means and methods have been investigated and employed to treat the inside surface of the glass plates which confine the LCs. Procedures include obliquely evaporated SiOx films,[1,2] mechanically rubbed polyimide layers,[3] electric field induced phase separation,[4,5] utilization of photoaligned, light sensitive, polymers,[6] Langmuir−Blodgett films,[7] lithographically micropatterned polymers,[8] and nanopatterned surfaces realized by using an atomic force microscope (AFM) or ion-beam etching surfaces.[9] Despite the availability of above-cited methods, the possibility of realizing a "surfactant free method" to align any kind of LC and self-organizing material is still an argument of ongoing research.

In this paper, we report on the detailed characterization of a new technique for aligning a wide range of LC materials that is based on an optical, multipurpose polymeric template. Without using any kind of surface chemistry, the distinctive intrinsic capability of the template to induce long-range order can be exploited for photonic applications, ranging from all-optical control of the diffraction efficiency of diffraction gratings based on LC, and containing photosensitive materials, to the ultra fast electro-optical switching of devices based on short pitch cholesteric LCs or surface stabilized LCs, to the realization of two-dimensional (2D) structures where the LC is confined in holes whose particular geometry determines the spatial orientation of the optical axis of the sample. We decided to perform new morphological, optical, all-optical, and electro-optical experiments to go deeper into the details of the extraordinary properties of our surfactant-free soft matter template. To this end, we have organized the present paper in different sections, in such a way that the most important novelties are highlighted with respect to preliminary results reported in a previous Communication.[10]

Received: November 7, 2012
Revised: January 4, 2013
Published: January 8, 2013

1. SOFT-COMPOSITE DIFFRACTION GRATINGS

In the last 20 years, great attention has been devoted to the possibility of exploiting LCs in confined structures, with particular attention to the realization of switchable holographic gratings. Research started from basic polymer dispersed liquid crystals (PDLCs),[11,12] indicating a droplet confined geometry, and led to the fabrication of switchable diffraction gratings named holographic polymer dispersed liquid crystals (HPDLCs).[13,14] These devices, while exhibiting good diffraction efficiency both in transmission and reflection,[15,16] can still present, in some particular case, some intrinsic drawback. In fact, if the droplet size of the nematic LC (NLC) component inside the polymeric matrix is comparable with the wavelength of the impinging light, the sample scatters the light. Reducing the average size of NLC droplets allows one to obtain higher diffraction efficiency and lower scattering losses, but the value of the electric field needed to induce a switching effect becomes rather high.[17,18] To overcome the mentioned drawback, some years ago, we realized a new kind of switchable diffraction grating, named POLICRYPS (acronym of "alternation of POLymer−LIquid CRYstal−Polymer Slices"), which is made of slices of almost pure polymer, alternated to films of well-aligned NLCs.[19−22] This composite structure is obtained by irradiating a homogeneous syrup of NLC (E7, by Merck) and prepolymer (NOA-61 by Norland, containing a UV sensitive photoinitiator), 28% and 72% in weight respectively, with an interference pattern of UV light, under suitable experimental and geometrical conditions. The curing process is carried out at a 100 nm precision level, by utilizing an optical holographic setup that enables the spatial periodicity of the structure to be easily varied from the almost nanometric to the micrometric range.[23,24]

The POM view of a POLICRYPS structure with a periodicity of $\Lambda = 5\ \mu m$, reported in Figure 1a, reflects the almost complete

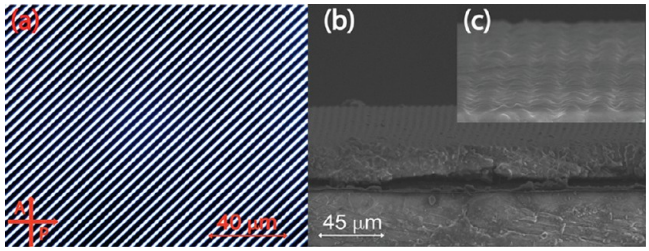

Figure 1. Polarized optical microscope (POM) micrograph (a) and ESEM side view (b), along with its high magnification (c) of a typical POLICRYPS structure.

phase separation that is usually achieved in this kind of systems and evidences the absence of LC droplets, whose presence could yield some scattering of the impinging light and some depolarization of the transmitted/diffracted one. Figure 1b is a side view of the POLICRYPS structure acquired by means of an environmental scanning electron microscope (ESEM) after removing the top cover glass. The analysis has been performed at the edge of the structure, after cutting the glass substrate along the middle of the sample. Usually, this operation is necessary for a side view analysis, in order to avoid viewing the nonuniform polymerization area that is present at the edge of the sample due to diffraction border effects. It is worth noting that the structure exhibits a morphology with a sinusoidal-like profile (high magnification Figure 1c), a topology that is due to the sinusoidal spatial modulation of the intensity of the curing interference pattern.

The POLICRYPS, which has been initially designed and utilized as a high quality, switchable, diffraction grating, was later exploited for several technological applications such as controllable wave-plate, Bragg filter, microlaser arrays, etc.[25,26] Despite results represent a breakthrough in comparison with similar advanced systems, some problem still remains. In fact, the single-step writing process of POLICRYPS gratings does not allow one to obtain high-quality results when exploiting novel, interesting effects in different self-organized materials (e.g., cholesteric LC, ferroelectric LC, azobenzene LC, etc.). Therefore, we have used the POLICRYPS morphology as a starting point for realizing a polymeric template with the capability of aligning a wide range of self-organizing materials.[10]

Optical Soft Matter Template. The basic POLICRYPS represents an excellent candidate to be used as a passive matrix for applications, due its unique morphological properties; in fact, the pure NLC confined between the polymeric slices can be easily removed in a selective way by exploiting a microfluidic etching process without opening the glass cell. In addition, the high quality morphology of the polymeric structure enables realizing a new generation of photonic devices. We have implemented a wet etching procedure of a POLICRYPS sample by immerging it (without opening the cell) in a water solution of tetrahydrofuran (THF) 50% in weight. This ratio has been chosen by taking into account: (i) the need to have a high boiling point (for the pure THF, it is 66 °C, while in our water solution it becomes 86 °C), at least above the nematic to isotropic transition of the used NLC (65 °C); (ii) the need to lower the viscosity of the pure THF (0.48 cP at 25 °C), which is a very important issue for realizing a microcapillary infiltration of the solution within the polymeric channels. Furthermore, the colorlessness of the solvent, and then of the solution, is very important to guarantee the optical transparence of the structure. In addition, THF is a moderately polar solvent (dipole moment ∼1.63 D) and can dissolve a wide range of nonpolar and polar (e.g., LCs) chemical compounds;[27] therefore, it represents the best candidate for realizing a selective microfluidic etching (driven by capillary forces) of the NLC that is inside the POLICRYPS. Indeed, after immerging the sample in the water solution of THF, the capillary flow starts washing out the LC confined in the polymeric channels: In a time interval of about 3−4 h (for 10 μm cell thickness and 5 μm fringe spacing), the THF acts as a selective agent and removes the LC and, eventually, any unpolymerized component, without affecting the regularity of the polymer slices. In general, however, the needed etching time depends on the geometry of the cell (thickness and fringe spacing), and a related characterization is reported in Table 1. The removing process is carried out above the nematic−isotropic transition temperature of the LC (65 °C), to ensure a low viscosity of this component, and is accelerated by vibrating the sample at

Table 1. Etching Time Interval Needed When Varying Thickness and Fringe Spacing of the Sample while Keeping Their Ratio Almost Constant

thickness (μm)	fringe spacing (μm)	etching time (hour)
1−5	1−5	8−9
6−10	6−10	3−4
11−16	11−16	1−2

dx.doi.org/10.1021/jp311027p | J. Phys. Chem. B 2013, 117, 1176−1185

ultrasonic frequency. Figure 2a clearly shows the effect of the microfluidic etching on a POLICRYPS structure: at first glance,

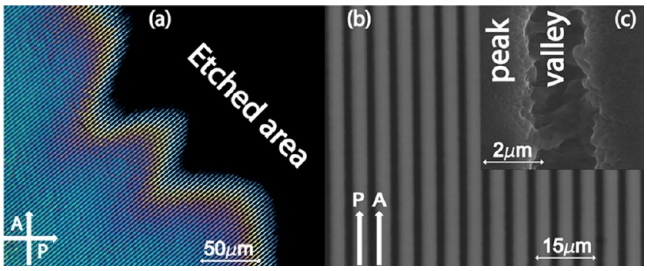

Figure 2. POM view of the POLICRYPS structure during the microfluidic etching process (a). Optical micrograph of the empty polymer template after removing the NLC (b) along with an ESEM view of a single channel (c). The modulation depth between the top of the polymeric slice (peak) and the bottom of the empty channel (valley) is about 10 μm.

the dark area indicates that the NLC has been washed out by the solvent. To confirm this hypothesis, we have performed an investigation of the "empty POLICRYPS" structure by observing the black area of Figure 2a between parallel polarizers (Figure 2b) with a high magnification objective (50×) of the microscope: the sample appears to be made of sharp polymer slices separated by empty channels. Then, we analyzed its morphology by an ESEM after removing, in this case, the top cover glass by means of a quite strong mechanical action (a process that affects the morphological quality of the structure); a view of a single channel is reported in Figure 2c. In this figure, it is evident that the edges of the polymeric channel are quite rough; this can be explained by considering, first, the aforementioned detachment of the top cover glass (the used photopolymer NOA 61 is an excellent glue for glass to glass bonding) and, second, the quite low intensity of the curing interference pattern at the edge of the bright fringe. Indeed, the polymerization process takes place in the high intensity region of the interference pattern with a consequent formation of very robust polymeric walls (peaks), while, due to the sinusoidal profile of the interference pattern, the process is weak on the edges of these walls and negligible in the middle of the empty channels (valley). For this reason, we believe the detachment of the top cover glass affects much more the edges of the polymeric walls. However, despite the apparently irregular morphology on these edges, it is important to notice that:

(a) We did not observe any polymeric scaffolding (or polymeric branches) that could, eventually, be present in the microchannel; this confirms the capability of the solvent to prevent this drawback.

(b) The channel is totally empty, which represents a clear confirmation that the LC has been completely removed. After the etching process has come to an end, and after leaving the sample on a hot plate for 12 h, which ensures the total evaporation of the solvent, thus avoiding the presence of NLC in the isotropic phase, we inspected the sample between the crossed polarizer of a POM, and we did not observe any residual birefringence (evaporating the solvent is an important step since the POM technique does not discern between an isotropic and a homogeneous medium).

(c) We characterized the empty polymeric channels (before removing the cover glass) by means of optical investigations (in terms of diffraction efficiency, angular selectivity, confocal analysis) and we did not observe any detectable scattering of the probing light or any fluorescence light; this is a clear confirmation that the roughness present in Figure 2c is mainly due to the removing process of the top cover glass, necessary to enable the ESEM analysis.

Finally, we want to stress that also photolithography or E-beam lithography allows realization of high quality photonic structures with nanoscale precision level. However, when we tried to align self-organizing materials in standard photoresist (SU8, AZ series, etc), only in the presence of a strong surface functionalization we have been able to observe a quite good alignment of NLCs, while we could not observe any alignment of other liquid crystalline components such as chiral LCs (CLCs) or ferroelectric LCs (FLC).

To conclude, the relevant result exposed in this section, also in comparison with the preliminary characterization reported in ref 10, is represented by the fact that, by performing an ESEM analysis of the polymeric structure before and after the etching process, we can confirm, on one hand, the good quality morphology of the POLICRYPS structure and, on the other hand, the absence of any liquid crystalline component after the etching process has come to the end.

2. ALL-OPTICAL DIFFRACTION GRATINGS

Noticeable attention has been recently devoted to the study of photoinduced phenomena in which the incident light brings molecular ordering or disordering in LC materials.[28−31] In particular, the realization of photonic systems in which light can be controlled by light represents the starting point for the implementation of high-speed all-optical devices.[32−34] Doping NLCs with photochromic molecules, such as azo-compounds, offers cheap, clean, and wireless control of the host mesophase properties, which depend mainly on the molecular director alignment of the mesogen. In this framework, the development of photoresponsive liquid crystals (PLCs) has provided outstanding solutions for all-optical switching applications. PLCs are, in general, LCs containing an azo group in their structure, thus exhibiting both the photosensitivity of azobenzene compounds and the birefringence of LCs. When acted on by UV or visible light, these materials undergo a reversible isomerization from a thermodynamically stable *trans* to a *cis* conformation, followed by a dramatic change in the macroscopic optical properties of the material.[35−37] The reverse transition can be obtained upon heating or irradiation with a different (longer wavelength) visible light (Figure 3). Depending on the wavelength and the time regime (CW or pulsed) of the impinging radiation, transition times can be varied from the nanosecond scale up to a few seconds.[38]

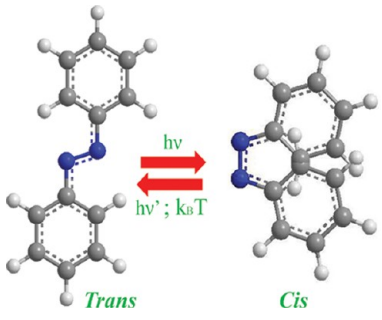

Figure 3. Schematic representation of the photoisomerization processes in the azobenzene molecule.

dx.doi.org/10.1021/jp311027p | J. Phys. Chem. B 2013, 117, 1176−1185

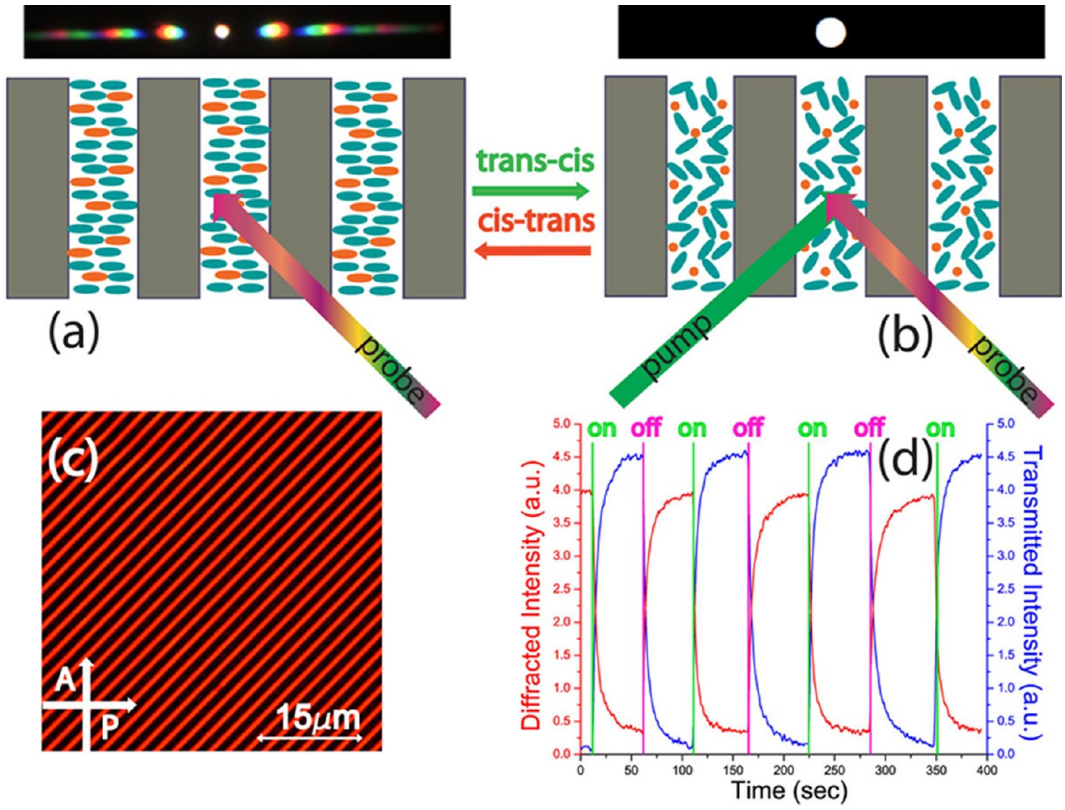

Figure 4. Photoisomerization processes taking place inside a POLICRYPS structure that undergoes different irradiation regimes (a,b). POM view of the polymeric template filled with azo-dye doped NLC (c), along with the all-optical response of the sample (d).

Recently, we have demonstrated that performances of PLCs are much better than the ones of LCs doped with non-mesogenic azo-dyes.[39] However, these last ones (such as Methyl Red (MR)) are commercial, low cost materials, and it might therefore be interesting to combine the polymeric template capability to induce long-range organization with the photosensitivity induced by these nonmesogenic azo-dyes. To this end, we have realized a light responsive LC by using a mixture containing common NLCs (E7, by Merck) doped with MR (2% in weight). To induce a long-range order in the material, we exploited the performances of our polymeric template; indeed, by capillary flow, we injected the mixture into the microchannels of the empty template according to the previously described method.[10] The diffraction properties of samples have been investigated by means of the standard pump−probe optical setup reported in detail in ref 39 and recalled in the Supporting Information.

The NLC orientation inside a POLICRYPS has been well characterized in the past, and it has been demonstrated that, despite the edges of the polymeric channels being quite rough, the NLC tends to align perpendicularly to the polymeric slices.[40] It is worth underlining that the exact composition of NOA-61 is still unknown, even if it should be a mix of a mercapto-ester with acrylate monomer as described elsewhere.[41] Thus, an explanation of the NLC alignment inside the polymeric channels can be found only in the following qualitative considerations: (a) NOA-61 is hydrophobic, with a contact angle of about 83°; the NLC possesses a hydrophobic alkyl chain and a hydrophilic cyano headgroup[42] and therefore tends to align perpendicularly to the hydrophobic part of the polymeric slices.[43] (b) NOA-61 is a thiol-based component,[40] and it has been already observed that the alkyl tails of the thiol induce a homeotropic alignment of the NLC, due to a covalent bonding.[44] Indeed, we performed experiments by realizing a uniform layer of NOA-61 and covering it with a NLC film: We observed a quite uniform NLC alignment. This confirms results reported in ref 44 concerning the covalent bonding between the alkyl tails of the thiol group present in the NOA-61 photopolymer and the NLC head. Here we note that one of the main drawbacks of a uniform NLC layer is the high sensitivity to temperature changes, which limits the field of possible applications. On the contrary, in the presence of the polymeric template: (i) the NLC is homogeneously aligned (due the aforementioned covalent bonding) and (ii) the NLC is very well stabilized due to the presence of the polymeric walls (confinement effect).

We stress that, in a recent paper,[45] a similar method has been reported, which was used to align NLCs in polydimethylsiloxane (PDMS) microfluidic channels; the NLC was injected by flow and homeotropically aligned to the PDMS channels without using any kind of surface chemistry. Despite the apparent similarity, in that case, a strong correlation between the homeotropic area and the cross-section of the channels has been observed; in particular, for channels with widths greater than their heights, NLC was perfectly aligned. When the height of the channel was comparable to its width, the alignment was inhomogeneous. In addition, the PDMS channels could align only NLC materials, while they required surface chemistry treatments for aligning other kind of LC phases (e.g., CLC, FLC, etc.). On the contrary, using the presented method, we have not observed any correlation between the NLC alignment area and the geometry of the channels; furthermore, we will show in the next section that we can align different LC phases as well, without using any surface treatment. Finally, we are sure

dx.doi.org/10.1021/jp311027p | J. Phys. Chem. B 2013, 117, 1176−1185

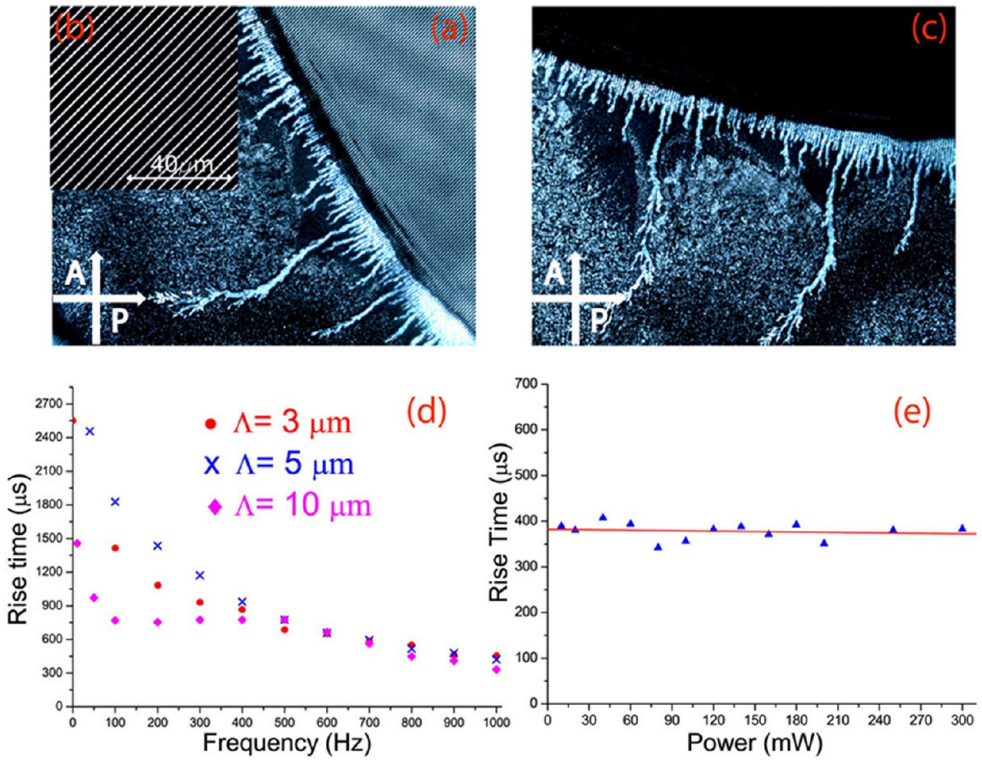

Figure 5. POM view of the template (grating vector aligned at 45° with the light polarization direction) filled with short pitch CLC at the edge of the grating area (a), and after rotating the grating vector of 45° (c). The high magnification of the CLC area aligned in ULH geometry is shown in panel b, along with its electro-optical characterization (d,e).

that, in the actual case, the alignment is due to the covalent bonding of the LC with the lateral surface of the empty microchannels, since on the top and bottom of the empty channels we used an untreated cover glass.

Figure 4a,b shows a schematic representation of the all-optical switching effect realized by varying the refractive index contrast of the polymeric template infiltrated with light responsive LCs (POM view, Figure 4c). By probing the sample with a multiline laser beam (Coherent, Innova 90C, p-polarized, Figure 4a) it is possible to observe the typical color diffraction pattern due to the high index contrast between the LC film and the polymeric slices, and a simple measurement of the diffracted intensities at different angles (different wavelengths) enables identifying the probing wavelength that maximizes the diffraction efficiency of the structure. When irradiating with a green pump laser over the spot of the multiline laser beam (Figure 4b), a trans−cis isomerization of the azo dye is induced, which affects the NLC order. In this condition, the probe beam experiences a LC average refractive index whose value is very close to the one of the polymer slices; thus, the diffracted intensity significantly decreases (with a corresponding increase of the transmitted intensity), since the structure exhibits an almost vanishing index contrast and becomes transparent to the impinging probe light (see the white transmission spot). As soon as the green pump beam is turned off, the probe light itself is able to induce a reverse (cis−trans) isomerization process, and the NLC order is restored.

We stress that we have performed experiments by varying the cross-section of the microchannels (from 0.4 to 15 μm in fringe spacing and from 2 to 25 μm in thickness), always obtaining a uniform and good alignment of the NLC. However, to check in details the all-optical characteristics of the structure, we have used a red probe laser (whose wavelength ensures a fast relaxation time to the trans conformation) and a grating with L = 7.8 μm thickness and Λ = 1.48 μm pitch; these values enable one to easily explore the morphology of the structure by means of a POM, while ensuring also that the highest diffraction efficiency is obtained with the red wavelength, in good agreement with the Kogelnik model.[46] Figure 4d shows the switching of both the diffracted (red curve) and the transmitted (blue curve) components of the p- polarized probe beam (λ = 633 nm, P_{probe}= 0.48 W/cm^2), driven by a sequence of on−off irradiance with pump green light (λ = 532 nm, P_{pump}= 57 mW/cm^2): the grating diffraction efficiency varies from 94% to 4%. In fact, these values are quite extreme for typical switchable gratings[47,48] and represent the demonstration of the high capability of our polymeric structure to induce molecular order in self-organizing materials (LCs), when they are not acted on by external perturbations.

The reasons we decided to characterize the optical response of our structures by using a quasi-random sequence (with an average duration of about 50 s) of the pump irradiance are as follows:

- This represents evidence that we are performing our experiments by using a real sequence of a pump beam, which is different from repeating a unique sequence several times.
- Usually, in our day life, we turn on and off devices in a random way; thus it is much more appropriate to realize scientific experiments with the same behavior.

Finally, we note that the response time of the on/off states changes when using a sequence of the pump beam with different time intervals. We believe this behavior is due to a degradation/instability of the nonmesogenic azo dye.[39] The

dx.doi.org/10.1021/jp311027p | J. Phys. Chem. B 2013, 117, 1176−1185

remarkable result reported in this section is represented by the realization of an all-optical control of light diffraction, operated by using a low cost and commercial photosensitive material. In our previous communication,[10] we used a high performance mesogenic azo-LC for realizing a light controllable diffraction grating, putting the accent on the mesogenic nature of the azo-compound. Now, we want to show the outstanding properties of our polymeric template: despite the intrinsic low performance of the material (nonmesogenic azo dye), we are able to obtain good alignment, very high diffraction efficiency and quite short response times. These achievements represent a step forward in comparison with similar structures fabricated by using the same material.[30−32]

3. UNIFORM LYING HELIX GEOMETRY

Modern technology based on conventional NLCs is limited by the viscoelastic effect, which yields typical "on" and "off" response times on the order of a few milliseconds or more. A few years ago, Patel and Meyer[49] showed that the flexoelectro-optic effect in CLCs can be used to obtain switching effects with submillisecond response times, although with weak optical phase modulation and the need of relatively high electric fields. In this framework, short pitch CLCs with uniform lying helixes (ULH) oriented in the plane of the layer have been studied in details.[50] The flexoelectric effect in CLCs, aligned in a ULH geometry, induces a tilt of the optical axis in the plane of the layer, with a tilt angle that linearly depends on the amplitude of the applied electric field. Despite the ULH texture exhibiting unique features, it usually needs to be stabilized by an external electric field since, otherwise, the texture tends to relax into a Grandjean configuration[51] over time. To overcome this drawback, several approaches for achieving a stable ULH texture have been studied, which include the realization of periodic anchoring conditions, or polymer stabilized network structures.[52] An interesting alternative approach consists in imposing confinement conditions that can enable the ULH formation at a low energy level. This can be obtained by the periodic presence of the polymeric slices of our empty template, which break the in-plane translational symmetry while imposing to the LC director an alignment perpendicular to the confining surfaces; in this geometry, the CLC helix can only orient along the polymeric channels.[53] In the first experiment, we used an indium tin oxide (ITO)-coated cell, $L = 10\ \mu$m in thickness and $\Lambda = 5\ \mu$m in spatial periodicity. The realized empty template has been filled by capillarity with BL088 CLC by Merck (helix pitch ∼400 nm) according to the previously described method.

Figure 5a is a POM micrograph of the sample at the edge of the photosculptured grating area, which shows, on the left, the existence of a standard focal conic texture, induced by a random distribution of the CLC helical axes. On the right, the ULH geometry induced by the polymeric structure is well evident (high magnification in Figure 5b). By rotating the sample of 45° under the microscope (Figure 5c), the appearance of the focal conic textures region (left) remains almost unchanged, while the ULH area (right) becomes almost dark, exhibiting a large contrast with the bright appearance of Figure 5a. This is the demonstration that a director alignment took place only in the ULH region. In order to perform the first electro-optical characterization, we mounted the sample on a rotating stage; the light from a He−Ne laser (λ=633 nm) passes through the polarizer, the sample, and the analyzer (whose optical axis is crossed with respect to the polarizer one) and finally is detected by a photodiode. The sample acts as a uniaxial retardation plate with its optical axis parallel to the direction of the microchannels; we placed it at 45° with respect to the polarizer/analyzer axes and monitored the transmitted intensity while applying an external electric field (square wave). In the ULH geometry, the electric field is applied perpendicular to the helix and induces an in-plane tilt of the optical axis with an angle that is proportional to the electric field;[54] the tilt is reversed when the polarity of the electric field is reversed. The transmitted intensity, which depends on the tilt of the optical axis,[54] results therefore proportional to the applied voltage. As already observed,[10] the response is linear with the applied field (up to 6.7 V/μm) with a characteristic time that falls in the microsecond range (Figure 5d). In order to verify the reliability of our technique, we have realized several samples with thickness $L = 10\ \mu$m, but different periodicity, ranging from 3 to 10 μm; all samples exhibited a well-ordered ULH texture, confirmed by the corresponding POM view. We measured (Figure 5d) the rise time while varying the frequency of the applied external field and keeping constant its amplitude (6.7 V/μm); we observed that, by increasing the frequency of the applied field, the rise time decreases from the millisecond to the microsecond range, following an exponential-like decay. This behavior can be explained by considering that, at low frequencies, the optical response has a mixed character with both a linear (flexoelectro-optic) and a quadratic (dielectric) dependence on the external field, since both amplitude and phase modulation of the transmitted light takes place; at high frequency, the electro-optic response is quite linear, since only the flexoelectric effect yields the major contribution to the response. As for the correlation between the response time and the periodicity of the sample (Figure 5d), we measured a quite significant difference only at low frequency (below 400 Hz). This difference can be explained by taking into account the effect of the free ions present inside the CLC. Indeed, at low frequency, the external electric field induces a migration of the free ions inside the microchannels; the internal electric field, which is created by this charge separation effect, reduces the helix tilt and therefore the corresponding response time. The effect is enhanced for large periodicity due to the high concentration of free ions that occurs in this case.

Finally, in order to check the robustness of the ULH stabilization induced by the polymeric slices of our structures, we measured the response time versus the power of the impinging probe beam, by exploiting a green laser light (λ = 532 nm) impinging on a sample with both spacing and thickness of 10 μm. The very small variations, which can be observed in Figure 5e, indicate that the stabilization action operated by the structure is able to overcome the increase of thermal noise produced by the increasing impinging intensity. Concluding this section, we point out the result presented here, which is represented by the detailed characterization of the ULH geometry, induced by the polymeric template, performed in terms of dependence on microchannel width and impinging probe power. Surprisingly, by lowering the frequency of the applied field, it is possible to exploit both quadratic (dielectric) and linear (flexoelectro-optic) electro-optical effects. This result, which has never been reported before, can really open up new ways for realizing a new generation of photonic devices (e.g., ULH-based LC displays) with submillisecond response times. In addition, our system does not exhibit the drawbacks that are typical of similar materials (e.g., probe intensity

dx.doi.org/10.1021/jp311027p | J. Phys. Chem. B 2013, 117, 1176−1185

dependence, strong temperature dependence and short lifetime).[50]

4. SURFACE STABILIZED FERROELECTRIC LIQUID CRYSTALS

FLC[55] materials can be exploited for the realization of fast electro-optical devices. They are characterized by an orientational order and a positional order of their molecules, which changes layer by layer. Molecules are indeed organized in a layered structure, with a molecular director axis tilted at a given angle (θ) with respect to the layer normal ($\hat{K}$). The existence of a spontaneous polarization is a microscopic property of a thin FLC film, while volume samples do not show, in general, any spontaneous polarization because of a helicoidal organization of the FLC molecules in the bulk: since the polarization vector changes with the helix, it averages to zero over the pitch length. In order to realize a bistable switching between two different polarized states, the helicoidal structure has to be unwound, and the most suitable way of doing this is to confine the FLC sample between two glass plates; in that case, the helicoidal structure is suppressed by the interaction with the boundary surfaces and the new sample geometry is named surface-stabilized FLC (SSFLC).[56] In this configuration, application across the cell of an external electric field causes a switching of the molecular director (**n**) around a cone, so that the spontaneous polarization (**P**) is brought to become aligned to the applied field. We decided to also explore the capability of our polymeric template to align FLCs. To this end, we have infiltrated the structure with CS-1024 FLC (by Chisso), always according to the previously described procedure.[10] We have analyzed several samples, all with a thickness $L = 10\ \mu$m, but different periodicity Λ, which was varied from 3 to 6 μm; the best results in terms of uniformity of the included SSFLC geometry (verified by POM analysis) were obtained in the sample with $\Lambda = (3 \pm 0.2)\ \mu$m and a corresponding channel width of about $(1.0 \pm 0.15)\ \mu$m, as sketched in Figure.6.

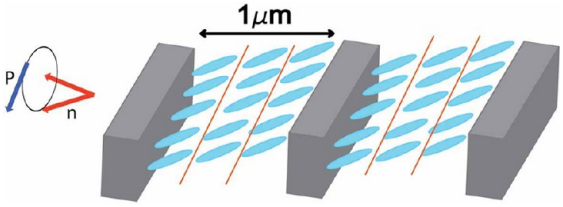

Figure 6. Sketch of the SSFLC geometry inside the polymeric template.

As a matter of fact, in this case, the helices undergo a restraint by the polymeric template channels whose width is of the same order of magnitude as the helical pitch: due to boundary conditions, **n** is constrained at a given angle (22°)[57] with the normal to the polymeric slices. We have investigated the electro-optical characteristics of our device by applying a bipolar pulse; we observed a variation of **n** (±22°) with a consequent variation of **P**, which is switched between two stable states (Clark–Lagerwall effect")[56] with typical response times that fall in the microsecond range.

Figure 7a is a POM micrograph of the sample at the edge of the grating area: it shows the typical conic texture of random aligned FLC molecules outside the grating area (right view) while a very well aligned SSFLC geometry is exhibited inside the grating area (left view). In order to have a deeper insight with respect to the results reported in our previous Communication,[10] we have analyzed the dynamics of the two stable states in terms of stability time; therefore, we monitored the intensity transmitted by the sample (in fact, by the area depicted in Figure 7a, left view) placed between crossed polarizers, when applying a single monopolar pulse. Results reported in Figure 7b show that the transmitted intensity (blue curve) is reduced by about 50% due to the switching of **n** (from +22° to −22°) with a consequent alignment of **P** (moving along a conic surface) to the direction of the electric field of the monopolar pulse (red curve). After the external field is turned off, the sample remains in a stable state for a time of about 1 ms; then the transmitted intensity is restored to its initial value in about 2 ms. These values strongly depend, however, on the geometry of the sample, and new efforts are necessary (in terms of new materials) for increasing the stability time, which is necessary for realizing high-performance devices. It is worth noting that we have used a 10 μm thick cell both for ULH and SSFLC geometries for minimizing the diffraction (and then maximizing the transmission) efficiency; indeed, according to the Kogelnik model,[46] the diffraction efficiency of a periodic structure can be varied from about 100% to about 0% by simply varying the thickness of the cell. Since devices based on the ULH and SSFLC effect exploit the transmission of the impinging light, the diffraction operated by the structure represents a drawback; we have therefore chosen a cell thickness that minimizes the diffraction efficiency of the sample.

We conclude this section by stating that we have characterized the dynamics of the SSFLC induced by the polymeric template and, in order to have a deeper insight with respect to previous reported results,[10] we have analyzed the dynamics of the stable states in terms of stability time, finding a memory time of a few milliseconds. This is one order of magnitude lower than the one observed in similar devices fabricated by using the same advanced materials,[56] and ongoing efforts are being devoted to further reduce this drawback.

5. 2D PERIODIC STRUCTURE

Up to now, we have shown exploitation of our POLICRYPS structure for the realization of one-dimensional (1D) electro-optical devices with application in the photonic field. One more interesting aspect is represented by the possibility of realizing 2D composite photonic devices.[58] First, we infiltrate the "empty POLICRYPS" structure with the same curing mixture used for the fabrication of 1D POLICRYPS. A 2D grid is then obtained by simply rotating the sample and following again the standard two-beam interference procedure utilized for the POLICRYPS fabrication, without the need of any multiple beam interference pattern. The versatility of this technique allows choosing the geometry of the unit cell of the grid; in particular, in addition to the typical, already reported, square hole geometry, obtained with a 90° rotation before operating of the second curing step,[59] here we report the fabrication of a "lozenge" hole geometry, obtained by a 45° rotation utilized for the second curing step. This geometry enables realization of microdomains with a strong asymmetry of the NLC director orientation, which turns out to be along the "lozenge" long diagonal, as verified by POM analysis.

Figure 8a shows the optical microscope view of this "lozenge hole" 2D POLICRYPS grid; the POM view of the NLC confined in the cavities (Figure 8c) shows an anisotropic configuration imposed by the local geometry. The optical characteristics of this configuration have been investigated by

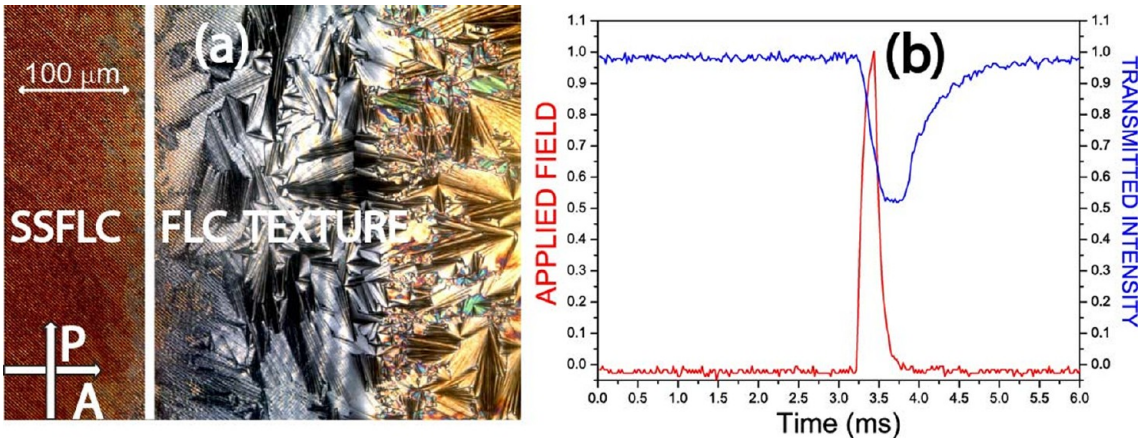

Figure 7. POM view of the POLICRYPS template filled with short pitch FLC at the edge of the grating area (a). The dynamics of the bistable electro-optical response is reported in (b).

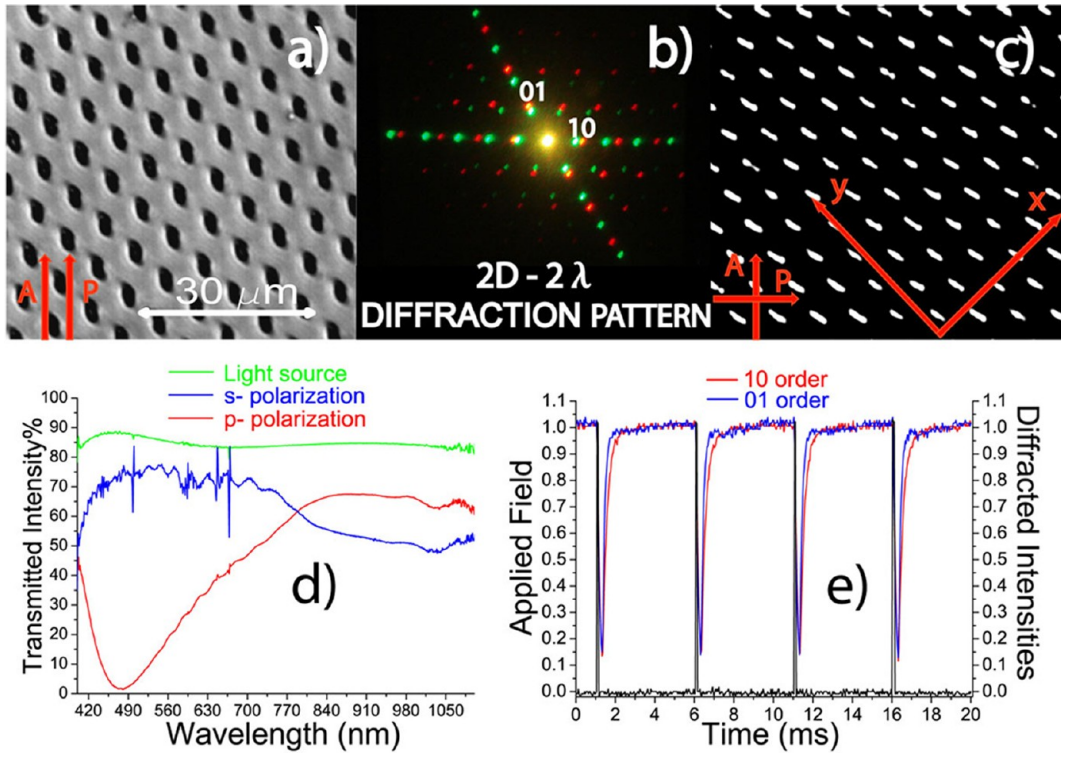

Figure 8. "Lozenge hole" 2D POLICRYPS grid (a); POM view of the NLC configuration (c); far-field diffraction pattern of two colaunched beams (b); spectral response (d); electro-optical response of the 10 and 01 diffracted orders (e) in terms of applied field and diffraction intensities, normalized to their maximum value.

means of an optical spectrometer, which enabled detection of polarized diffraction spectra; Figure 8d shows the transmission of the sample for two orthogonal impinging polarizations: p-polarized light experiences a large refractive index modulation (since $n_p \neq n_e$, where n_p and n_e are the polymer and the NLC extraordinary refractive indices, respectively), as shown in Figure 8b by the far field diffraction pattern of two colaunched beams. The transmitted wave exhibits, therefore, a band gap due to the strong diffraction operated by the 2D structure in this spectral range (red curve). On the contrary, s-polarized light (polarization along the x axis) experiences a low index modulation (since $n_p \sim n_o$, where n_o is the NLC ordinary refractive index) and the transmitted light exhibits a spectrum (blue curve) whose shape is similar to the impinging light one (green curve). We have investigated the electro-optical response of our 2D-POLICRYPS grid by exploiting a low frequency (1 kHz) square-wave voltage (Epp= 8.9 V/μm). Results are shown in Figure8e, where some switching cycles of the diffracted intensity (10 and 01 orders) are shown as obtained by switching "on" and "off" the external electric field. The plot is the demonstration that our 2D-POLICRYPS grid can be electrically controlled with response times that fall in the millisecond range. However, it is necessary to mention that, during the second curing step, the LC is subject to a microdiffusion process within polymeric channels. For this reason, we observed a deterioration of the quality of the sample (in terms of uniform alignment) below 1.5 μm of channel width. One way to minimize this effect can be tried by

dx.doi.org/10.1021/jp311027p | J. Phys. Chem. B 2013, 117, 1176−1185

increasing the curing temperature or by using a new generation of LCs materials (e.g., low viscosity). This solution might allow the realization of 2−3D structure with short periodicity.

It is worth noting that here we report on the first photonic band gap behavior that is based on a diffractive mechanism in a new kind of 2D photonic structure, with a "lozenge" hole geometry. Despite the need of a multistep process, this geometry enables realization of microdomains with a strong asymmetry in the NLC director orientation, which turns out to be along the "lozenge" long diagonal; in this way, observation of a photonic band gap can be controlled by simply choosing a suitable polarization of the impinging light. This result enables a new way to realize photonic devices based on the exploitation of diffraction efficiency as an active mechanism for preventing or enabling the propagation of light.

CONCLUSIONS

We have exploited a new way for aligning liquid crystalline materials without using any kind of surface treatment. An empty polymeric microstructure has been realized by combining a holographic optical setup and a chemical etching process; the structure proved suitable to be employed for inducing long-range order in several kinds of liquid crystalline materials. In particular, NLCs doped with photosensitive molecules have been used for realizing a diffraction grating where an all-optical control of the diffraction of light can be operated. Short pitch CLCs, aligned in a ULH, and FLCs, in a SSFLC geometry, have been exploited for demostrating an ultrafast photonic switch. Finally, a versatile 2D refractive structure consisting of highly anisotropic NLC microdomains confined inside well-sculptured lozenge cavities has been fabricated. The capability of our surfactant free polymeric template to induce self-organization represents an opening for realizing a new generation of smart photonic devices where micro/nanotechnology meets self-assembly.

ASSOCIATED CONTENT

Supporting Information

All-optical setup for characterizing the diffraction properties of the light sensitive LC confined in the polymeric template. This information is available free of charge via the Internet at http://pubs.acs.org/.

AUTHOR INFORMATION

Corresponding Author

*E-mail: luciano.desio@fis.unical.it.

Notes

The authors declare no competing financial interest.

ACKNOWLEDGMENTS

The authors are grateful to Dr. Giovanni Desiderio for his help in the ESEM analysis and Dr. Loredana Ricciardi for drafting the artwork on the photoisomerization process (Figure 3). L.D. and C.U. acknowledge the NANOGOLD project (Seventh Framework Programme Theme, NMP-2008-2.2-2, Nanostructured metamaterials Grant Agreement No. 228455) for partial financial support.

REFERENCES

(1) Janning, J. L. Thin Film Surface Orientation for Liquid Crystals. *Appl. Phys. Lett.* **1972**, *21*, 173−174.
(2) Cognard, J. Alignment of Nematic Liquid-Crystals and Their Mixtures. *Mol. Cryst. Liq. Cryst.* **1982**, *1*, 1−78.
(3) Bahadur, B. Liquid Crystal Displays. *Mol. Cryst. Liq. Cryst.* **1984**, *109*, 3−93.
(4) Ren, H.; Wu, S. T.; Lin, Y. H. Single Glass Substrate Liquid Crystal Device Using Electric Field Enforced Phase Separation and Photoinduced Polymerization. *Appl. Phys. Lett.* **2007**, *90*, 191105−191107.
(5) Ren, H.; Wu, S. T.; Lin, Y. H. In-Situ Observation of Fringing Field-Induced Phase Separation in a Liquid Crystal and Monomer Mixture. *Phys. Rev. Lett.* **2008**, *100*, 117801−117804.
(6) Jain, S. C.; Kitzerow, H. S. Bulk Induced Alignment of Nematic Liquid Crystal by Photopolymerization. *Appl. Phys. Lett.* **1994**, *64*, 2946−2948.
(7) Barbero, G. A.; Petrov, G. Nematic Liquid Crystal Anchoring on Langmuir-Blodgett Films: Steric, Dielectric and Flexoelectric Aspects and Instabilities. *J. Phys. Condens. Matter.* **1994**, *6*, 2291−2306.
(8) Pidduck, A. J.; Haslam, S. D.; Bryan-Broan, G. P.; Bannister, R.; Kitely, I. D. Control of Liquid Crystal Alignment by Polyimide Surface Modification Using Atomic Force Microscopy. *Appl. Phys. Lett.* **1997**, *71*, 2907−2909.
(9) Chaudhari, P.; Lacey, J.; Doyle, J.; Galligan, E.; Lien, S. C. A.; Callegari, A.; Hougham, G.; Lang, N. D.; Andry, P. S.; John, R.; et al. Atomic-Beam Alignment of Inorganic Materials for Liquid-Crystal Displays. *Nature* **2001**, *411*, 56−59.
(10) De Sio, L.; Ferjani, S.; Strangi, G.; Umeton, C.; Bartolino, R. Universal Soft Matter Template for Photonic Applications. *Soft Matter* **2011**, *7*, 3739−3743.
(11) Ferguson, J. L. Polymer Encapsulated Nematic. Liquid Crystals for Display and Light Control. Applications. *Proc. Int. Symp. Dig. Tech. Pap. (SID '85)* **1985**, *16*, 68−70.
(12) Doane, J. W.; Vaz, B. G.; Wu, N. A.; Žumer, S. Field Controlled Light Scattering from Nematic Microdroplets. *Appl. Phys. Lett.* **1986**, *48*, 269−271.
(13) Margerum, J. D.; Lackner, A. M.; Ramos, E.; Smith, G. W.; Vaz, N. A.; Kohler, J. L.; Allison, C. R. Polymer Dispersed Liquid Crystal Film Devices. U.S. patent 5096282 (March 17, 1992).
(14) Natarajan, L. V.; Sutherland, R. L.; Tondiglia, V. P.; Bunning, T. J.; Adams, W. W. Electro-optical Switching Characteristics of Volume Holograms in Polymer Dispersed Liquid Crystals. *J. Nonlinear Opt. Phys. Mater.* **1996**, *5*, 89−98.
(15) Bunning, T. J.; Natarajan, L. V.; Sutherland, R. L.; Tondiglia, V. P. Holographic Polymer-Dispersed Liquid Crystals (H-PDLCs). *Annu. Rev. Mater. Sci.* **2000**, *30*, 83−115.
(16) Sutherland, R. L.; Natarajan, L. V.; Tondiglia, V. P.; Bunning, T. J. Volume Hologram Formation in Liquid-Crystal/Photopolymer Mixtures. *SPIE Proc* **2003**, *5003*, 35−43.
(17) Lucchetta, D. E.; Karapinar, R.; Manni, A.; Simoni, F. Phase-Only Modulation by Nanosized Polymer Dispersed Liquid Crystals. *J. Appl. Phys.* **2002**, *91*, 6060−6065.
(18) Castagna, R.; Vita, F.; Lucchetta, D. E.; Criante, L.; Simoni, F. Superior-Performance Polymeric Composite Materials for High-Density Optical Data Storage. *Adv. Mater.* **2009**, *21*, 589−592.
(19) Caputo, R.; De Sio, L.; Veltri, A.; Umeton, C.; Sukhov, A. V. Development of a New Kind of Switchable Holographic Grating Made of Liquid-Crystal Films Separated by Slices of Polymeric Material. *Opt. Lett.* **2004**, *29*, 1261−1263.
(20) Caputo, R.; Veltri, A.; Umeton, C. P.; Sukhov, A. V. Characterization of the Diffraction Efficiency of New Holographic Gratings with a Nematic Film−Polymer-Slice Sequence Structure. *J. Opt. Soc. Am. B* **2004**, *21*, 1939−1947.
(21) Caputo, R.; Sukhov, A. V.; Umeton, C.; Veltri, A. Kogelnik-like Model for the Diffraction Efficiency of POLICRYPS Gratings. *J. Opt. Soc. Am. B* **2005**, *22*, 735−742.
(22) Veltri, A.; Caputo, R.; Sukhov, A. V.; Umeton, C. Model for the Photoinduced Formation of Diffraction Gratings in Liquid-Crystalline Composite Materials. *Appl. Phys. Lett.* **2004**, *84*, 3492−3494.
(23) De Sio, L.; Caputo, R.; De Luca, A.; Veltri, A.; Umeton, C.; Sukhov, A. V. In Situ Optical Control and Stabilization of the Curing

Process of Holographic Gratings with a Nematic Film−Polymer-Slice Sequence Structure. *Appl. Opt.* **2006**, *45*, 3721−3727.
(24) De Sio, L.; Veltri, A.; Tedesco, A.; Caputo, R.; Umeton, C.; Sukhov, A. V. Characterization of an Active Control System for Holographic Setup Stabilization. *Appl. Opt.* **2008**, *47*, 1363−1367.
(25) Caputo, R.; De Sio, L.; Veltri, A.; Umeton, C.; Sukhov, A. V. POLICRYPS Switchable Holographic Grating: A Promising Grating Electro-optical Pixel for High Resolution Display Application. *J. Disp. Technol.* **2006**, *2*, 38−51.
(26) Caputo, R.; De Luca, A.; De Sio, L.; Pezzi, L.; Strangi, G.; Umeton, C.; Veltri, A.; Asquini, A.; d'Alessandro, A.; Donisi, D.; et al. POLICRYPS: A Liquid Crystal Composed Nano-microstructure with a Wide Range of Optical and Electro-optical Applications. *J. Opt. A: Pure Appl. Opt.* **2009**, *11*, 024017−024030.
(27) Belandria, V.; Mohammadi, A. H.; Richon, D. Volumetric Properties of the (Tetrahydrofuran+Water) and (Tetra-*n*-butyl Ammonium Bromide+Water) Systems: Experimental Measurements and Correlations. *J. Chem. Thermodyn.* **2009**, *41*, 1382−1386.
(28) Lee, H. K.; Kanazawa, A.; Shiono, T.; Ikeda, T. All-Optically Controllable Polymer/Liquid Crystal Composite Films Containing the Azobenzene Liquid Crystal. *Chem. Mater.* **1998**, *10*, 1402−1407.
(29) Shishido, A.; Kanazawa, A.; Shiono, T.; Ikeda, T.; Tamai, N. Enhancement of Stability in Optical Switching of Photosensitive Liquid Crystal by Means of Reflection-Mode Analysis. *J. Mater. Chem.* **1999**, *9*, 2211−2214.
(30) Khoo, I. C.; Chen, P. H.; Shih, M. Y.; Shishido, A.; Slussarenko, S.; Wood, M. V. Supra Optical Nonlinearities (SON) of Methyl Red- and Azobenzene Liquid Crystal-Doped Nematic Liquid Crystals. *Mol. Cryst. Liq. Cryst.* **2001**, *358*, 1−13.
(31) Urbas, A.; Tondiglia, V.; Natarajan, L.; Sutherland, R.; Yu, H.; Li, J. H.; Bunning, T. Optically Switchable Liquid Crystal Photonic Structures. *J. Am. Chem. Soc.* **2004**, *126*, 13580−13581.
(32) Ikeda, T.; Tsutsumi, O. Optical Switching and Image Storage by Means of Azobenzene Liquid-Crystal Films. *Science* **1995**, *268*, 1873−1875.
(33) Gupta, M. C. *Handbook of Photonics*; CRC Press: New York, 1997.
(34) Khoo, I. C. Nonlinear Optics of Liquid Crystalline Materials. *Phys. Rep.* **2009**, *471*, 221−267.
(35) Tsutsumi, O.; Kanazawa, A.; Shiono, T.; Ikeda, T.; Park, L. S. Photoinduced Phase Transition of Nematic Liquid Crystals with Donor-Acceptor Azobenzenes: Mechanism of the Thermal Recovery of the Nematic Phase. *Phys. Chem. Chem. Phys.* **1999**, *1*, 4219−4224.
(36) Hrozyk, U. A.; Serak, S. V.; Tabiryan, N. V.; Hoke, L.; Steeves, D. M.; Kimball, B.; Kedziora, G. Systematic Study of Absorption Spectra of Donor−Acceptor Azobenzene Mesogenic Structures. *Mol. Cryst. Liq. Cryst.* **2008**, *489*, 257−272.
(37) Hrozhyk, U. A.; Serak, S. V.; Tabiryan, N. V.; Hoke, L.; Steeves, D. M.; Kimball, B. R. Azobenzene Liquid Crystalline Materials for Efficient Optical Switching with Pulsed and/or Continuous Wave Laser Beams. *Opt. Express* **2010**, *18*, 8697−8704.
(38) De Sio, L.; Veltri, A.; Umeton, C.; Serak, S.; Tabirian, N. All-Optical Switching of Holographic Gratings Made of Polymer-Liquid-Crystal-Polymer Slices Containing azo-Compound. *Appl. Phys. Lett.* **2008**, *93*, 181115−181117.
(39) De Sio, L.; Serak, S.; Tabiryan, N.; Umeton, C. Mesogenic versus non-Mesogenic azo Dye Confined in a Soft-Matter Template for Realization of Optically Switchable Diffraction Gratings. *J. Mater. Chem.* **2011**, *21*, 6811−6814.
(40) Castriota, M.; Fasanella, A.; Cazzanelli, E.; De Sio, L.; Caputo, R.; Umeton, C. In Situ Polarized Micro-Raman Investigation of Periodic Structures Realized in Liquid-Crystalline Composite Materials. *Opt. Express* **2011**, *19*, 10494−10500.
(41) Pinto-Iguanero, B.; Olivares-Perez, A.; Fuentes-Tapia, I. Holographic Material Film Composed by Norland Noa 65® Adhesive. *Opt. Mater.* **2002**, *20*, 225−232.
(42) Kossyrev, P. A.; Yin, A.; Cloutier, S. G.; Cardimona, D. A.; Huang, D.; Alsing, P. M.; Xu, J. M. Electric Field Tuning of Plasmonic Response of Nanodot Array in Liquid Crystal Matrix. *Nano Lett.* **2005**, *5*, 1978−1981.
(43) Choi, M. C.; Pfohl, T.; Wen, Z.; Li, Y.; Kim, M. W.; Israelachvili, J. N.; Safinya, C. R. Ordered Patterns of Liquid Crystal Toroidal Defects by Microchannel Confinement. *Proc. Natl Acad. Sci. U.S.A.* **2004**, *101*, 17340−17344.
(44) Hoogboom, J.; Rasing, T.; Rowan, A. E.; Nolte, R. J. M. LCD Alignment Layers. Controlling Nematic Domain Properties. *J. Mater. Chem.* **2006**, *16*, 1305−1314.
(45) Cuennet, J. G.; Vasdekis, A. E.; De Sio, L.; Psaltis, D. Optofluidic Modulator Based on Peristaltic Nematogen Microflows. *Nat. Photonics* **2011**, *5*, 234−238.
(46) Kogelnik, H. Coupled Wave Theory for Thick Hologram Gratings. *Bell Syst. Tech. J.* **1969**, *48*, 2909−2947.
(47) Urbas, A.; Klosterman, J.; Tondiglia, V.; Natarajan, L.; Sutherland, R.; Tsutsumi, O.; Ikeda, T.; Bunning, T. Optically Switchable Bragg Reflectors. *Adv. Mater.* **2004**, *16*, 1453−1456.
(48) Lucchetta, D. E.; Vita, F.; Simoni, F. All-Optical Switching of Diffraction Gratings Infiltrated with Dye-Doped Liquid Crystals. *Appl. Phys. Lett.* **2010**, *97*, 231112−231112.
(49) Patel, J. S.; Meyer, R. B. Flexoelectric Electro-optics of a Cholesteric Liquid Crystal. *Phys. Rev. Lett.* **1987**, *58*, 1538−1540.
(50) Meyer, R. B. Piezoelectric Effects in Liquid Crystals. *Phys. Rev. Lett.* **1969**, *22*, 918−921.
(51) Sauper, A.; Meyer, G. Structure of Reflection Bands of Grandjean Textures. *Phys. Rev. A* **1983**, *27*, 2196−2200.
(52) Carbone, G.; Corbett, D.; Elston, S. J.; Raynes, P.; Jesacher, A.; Simmonds, R.; Booth, M. Uniform Lying Helix Alignment on Periodic Surface Relief Structure Generated via Laser Scanning Lithography. *Mol. Cryst. Liq. Cryst.* **2011**, *544*, 37−49.
(53) Carbone, G.; Salter, P.; Elston, S. J.; Raynes, P.; De Sio, L.; Ferjani, S.; Strangi, G.; Umeton, C.; Bartolino, R. Short Pitch Cholesteric Electro-optical Device Based on Periodic Polymer Structures. *Appl. Phys. Lett.* **2009**, *95*, 011102−011104.
(54) Broughton, B. J.; Clarke, M. J.; Blatch, A. E.; Coles, H. J. Optimized Flexoelectric Response in a Chiral Liquid-Crystal Phase Device. *J. Appl. Phys.* **2005**, *98*, 034109.
(55) Gennes, P. G. D.; Prost, J. *The Physics of Liquid Crystals*, 2nd ed.; Oxford University Press: United Kingdom, 1995.
(56) Clark, N. A.; Lagerwall, S. T. Submicrosecond Bistable Electro-optic Switching in Liquid Crystals. *Appl. Phys. Lett.* **1980**, *36*, 899−901.
(57) Lee, J. B.; Pelcovits, R. A.; Meyer, R. B. Role of Electrostatics in the Texture of Islands in Free-Standing Ferroelectric Liquid Crystal Films. *Phys. Rev. E: Stat., Nonlinear, Soft Matter Phys.* **2007**, *75*, 051701−051706.
(58) Yablonovitch, E. Inhibited Spontaneous Emission in Solid-State Physics and Electronics. *Phys. Rev. Lett.* **1987**, *58*, 2059−2062.
(59) De Sio, L.; Umeton, C. Dual-Mode Control of Light by Two-Dimensional Periodic Structures Realized in Liquid-Crystalline Composite Materials. *Opt. Lett.* **2010**, *35*, 2759−2761.